Vibrational spectroscopy at high pressures. 54. Decacarbonyldimanganese and decacarbonyldirhenium



1991 J. Phys.: Condens. Matter 3 6145

(http://iopscience.iop.org/0953-8984/3/32/019)

J. Phys.: Condens. Matter 3 (1991) 6145–6158. Printed in the UK

# Vibrational spectroscopy at high pressures: part 54. Decacarbonyldimanganese and decacarbonyldirhenium

David M Adams, Peter D Hatton† and Andrea C Shaw
Department of Chemistry, University of Leicester, Leicester LE1 7RH, UK

Received 21 February 1991, in final form 23 April 1991

**Abstract.** Raman spectra of $Mn_2(CO)_{10}$ and $Re_2(CO)_{10}$ have been studied to 27 and 98 kbar respectively, and the infrared (IR) spectrum of $Re_2(CO)_{10}$ to 30 kbar at ambient temperature. Both materials undergo a first-order structural phase transition at high pressure (Mn at approximately 8 kbar, Re at approximately 5 kbar) which is accompanied by dramatic changes in all regions of their vibrational spectra. These data are interpreted in terms of a change of molecular geometry from $D_{4d}$ to $D_{4h}$. In the new high-pressure phases the M to carbonyl backbonding is increased significantly for the axial but not the equatorial carbonyls. The molecular torsion is implicated in the phase change but is not thought to drive it.

## 1. Introduction

Many phase transitions are known in organic molecular materials but much less attention has been paid to those composed of inorganic molecules. We report a high-pressure study of the title compounds, $Mn_2(CO)_{10}$ and $Re_2(CO)_{10}$. A metal–metal bond links the two halves of the molecule, and the possibility of torsion about this bond holds the prospect of a phase transition analogous to that shown by biphenyl (Ponte-Goncalves 1980). Apart from our own preliminary account of this work (Adams *et al* 1981), these materials have not been studied at elevated pressures, apart from an investigation of their electronic spectra to 120 kbar (Carroll *et al* 1985). These workers did not observe the phase transitions we report because their method was sensitive only to changes from cylindrical symmetry and, as we show later, both structures involved in the phase transition are cylindrical.

## 2. Experimental procedure

Commercial samples of the metal carbonyls were purified by resublimation before use. Infrared spectra were obtained with a Perkin–Elmer 580B spectrometer and Raman spectra with a Coderg T800 instrument. High-pressure spectra were recorded using a diamond anvil cell (DAC), pressures being estimated by the ruby *R*-line method (Piermarini and Block 1975, Adams *et al* 1976). A simple refracting beam condenser was used with the DAC for the IR work. Inconel gaskets were used in the DAC with

† Present address: Department of Physics, University of Edinburgh, Edinburgh EH9 3JZ, Scotland.

0953-8984/91/326145+14$03.50  

initial thickness and hole diameter of 0.05 and 0.50 mm respectively. Corresponding dimensions for Raman studies were 0.20 and 0.40 mm. The pressure-transmitting fluid used was Nujol; this freezes at 13 kbar but remains plastic. Some work was also done in 4:1 methanol:ethanol but there were signs of reaction with the samples under these conditions. The samples were used as microcrystalline powders. Results from several different loadings indicated the absence of polarization effects due to crystallite orientation. Raman spectra were stimulated with 70 mW (at the sample) of 514.5 nm radiation: there were no signs of decomposition at these powers.

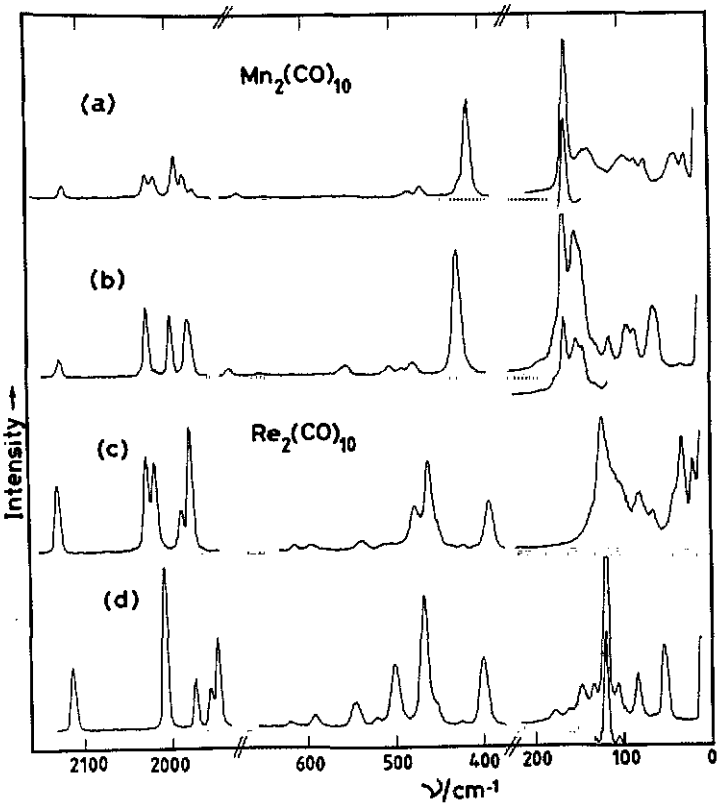


**Figure 1.** Raman spectra of $Mn_2(CO)_{10}$ at (*a*) ambient pressure, (*b*) 16 kbar and of $Re_2(CO)_{10}$ at (*c*) ambient pressure, (*d*) 16 kbar, in a diamond anvil cell.

## 3. Results and discussion

These compounds are isomorphous, consisting of discrete molecules packed in a monoclinic unit cell ($I2/a$ or $C2/c$) (Dahl *et al* 1957, Churchill *et al* 1981). They contain a single metal–metal bond with five terminal carbonyl groups completing an octahedral environment about each metal atom. There are no bridging carbonyl groups as, for example, in $Fe_2(CO)_9$ (Powell and Evans 1939, Cotton and Troup 1974). The two sets of equatorial carbonyl groups are in staggered configuration, resulting in approximately $D_{4d}$ overall symmetry.

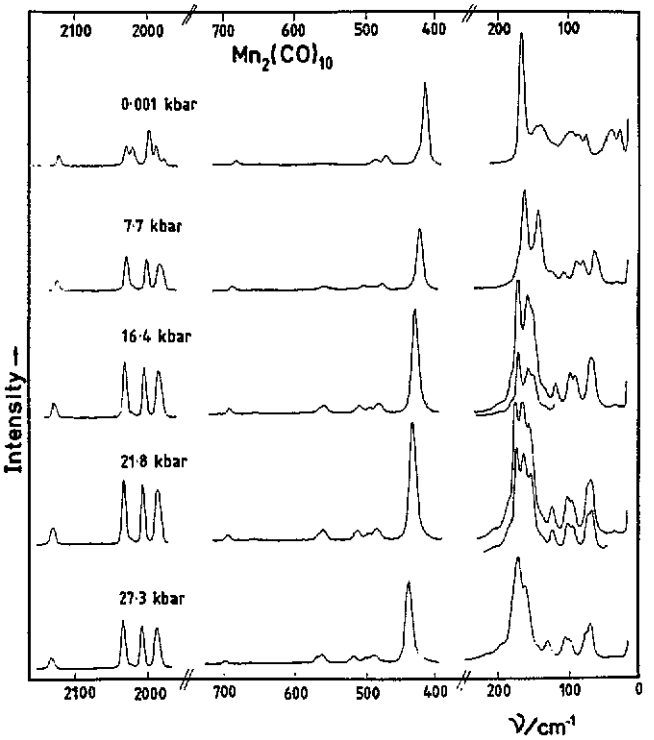


**Figure 2.** Raman spectra of $Mn_2(CO)_{10}$ at high pressures in a diamond anvil cell.

### *3.1. The phase behaviour*

Neither material shows a phase change upon cooling to liquid nitrogen temperature (Martin *et al* 1982, Harvey and Butler 1985): both undergo phase transitions at elevated pressures. In a DAC used without a gasket between the anvils there is a pressure gradient on the sample from maximum at the anvil centre to zero at the edge. This shear stress may be used to reveal phase changes by means of any associated refractive index discontinuity, forming a so-called Becke line. Manganese carbonyl is light yellow–orange under ambient conditions but at low applied pressures transforms sharply to a dark yellow form. Further pressure increase resulted in very slight darkening but gave no sign of another phase change to pressures of at least 150 kbar.

Rhenium carbonyl is white, but a faint Becke line can be seen at low applied pressures. After this phase change, to higher pressures, both our Raman results and the electronic spectra of Carroll *et al* (1985) showed no sign of a further structural change to 120 kbar.

Under hydrostatic conditions within a gasketed DAC, dramatic changes were observed in the Raman spectra, indicative of structural phase changes, figures 1 to 7. Data on the mode shifts with pressure are given in tables 1 to 4.

The phase changes we have discovered in these systems show hysteresis. Thus, for $Mn_2(CO)_{10}$ traces of the ambient phase (I) could still be detected at 20 kbar on initial increase of pressure, whereas on descending from high pressure phase II was retained until about 7.7 kbar. Major changes in all regions of the vibrational spectrum accompany the phase change, figures 1 to 3; and many of the mode plots show discontinuities, figures 4 to 7. These criteria establish the transitions as first-

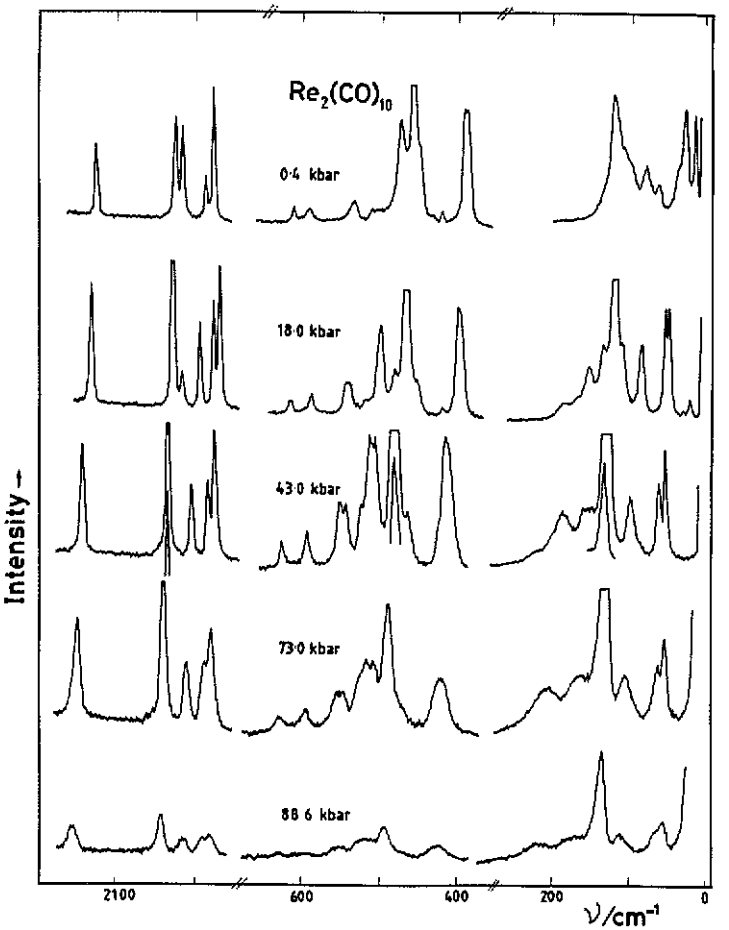


**Figure 3.** Raman spectra of $Re_2(CO)_{10}$ at high pressures in a diamond anvil cell.

order in type. For $Mn_2(CO)_{10}$ the transition is near 8 kbar and for $Re_2(CO)_{10}$ near 5 kbar. We base our discussion primarily upon $Re_2(CO)_{10}$ as our data are more extensive for it than for $Mn_2(CO)_{10}$. Changes in the lattice mode region are expected when a molecular crystal is repacked. What is unusual in the present case is the extent of the changes in all regions of the spectrum, internal and external modes. These are such as to imply that a change in molecular geometry accompanies the phase transition. A torsional distortion about the M–M bond will be of low energy: therefore we investigate the effect of a change from the initial staggered ($D_{4d}$) shape to the eclipsed ($D_{4h}$) form, as in figure 8.

The mode numbering scheme is given in table 5, and the correlations for the unit cell of phase I in table 6.

### *3.2. The (CO) region*

The $\nu$(CO) region of solid $Re_2(CO)_{10}$ has been assigned in detail on the basis of single-crystal Raman experiments (Adams and Hooper 1979) and is known to consist of four Raman-active modes: $A_1, \nu_1 > E_2, \nu_{25} > E_3$, $\nu_{31}$; $A_1, \nu_2$. The unit cell is monoclinic ($C2/c = C_{2h}^6$, $z = 4$) with a bimolecular primitive cell in which the molecules are on $C_2$ sites. Accordingly the degeneracy of the $E_2$ and $E_3$ modes is lifted yielding, in

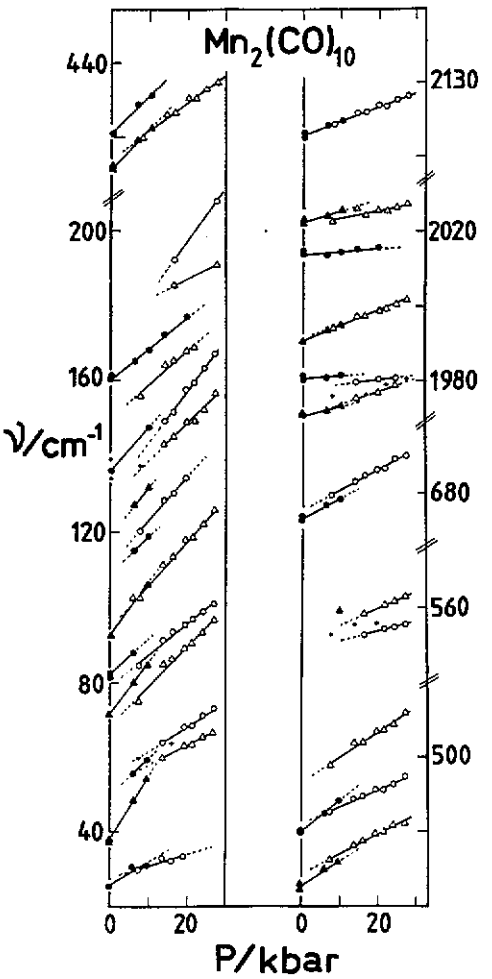


**Figure 4.** Pressure dependencies of the Raman-active modes of $Mn_2(CO)_{10}$.

each case, a vector: $A_g + B_g + A_u + B_u$, table 1. Hence, each mode ($\nu_{25}$,$\nu_{31}$) yields a Raman-active doublet, and this splitting is seen clearly under ambient conditions, figure 1. On entering phase II the $E_2$ doublet at 2027, 2018 cm$^{-1}$ collapses to a single band but there is no change in the number of bands which arise from the other $\nu$(CO) modes. This is precisely what is expected on the basis of a change to $D_{4h}$ rules, table 7: the $E_2(D_{4d})$ species becomes $B_{1g}$(Raman) + $B_{2u}$(inactive) in $D_{4h}$. At the phase transition it appears as if there is an increase in the number of bands below 2000 cm$^{-1}$ from two to three. However, the lower of these bands in the ambient phase is known to be due to near-coincidence of $A_1, \nu_2$ with the $B_g$ factor group component of $E_3, \nu_{31}$: at the transition these two modes move apart by 8 cm$^{-1}$, the lower one probably being associated with $\nu_2$. This is seen clearly in figure 1.

For $Mn_2(CO)_{10}$ the behaviour of $E_2, \nu_{25}$ mirrors that in the rhenium compound. However, the two $E_3, \nu_{31}$ components and $A_1, \nu_2$ are all clearly seen under ambient conditions. At the transition there is no discontinuous change in $\nu_2$ and, in further contrast to $Re_2(CO)_{10}$, the two factor group components of $E_3$ move together with increasing pressure, figures 2 and 4.

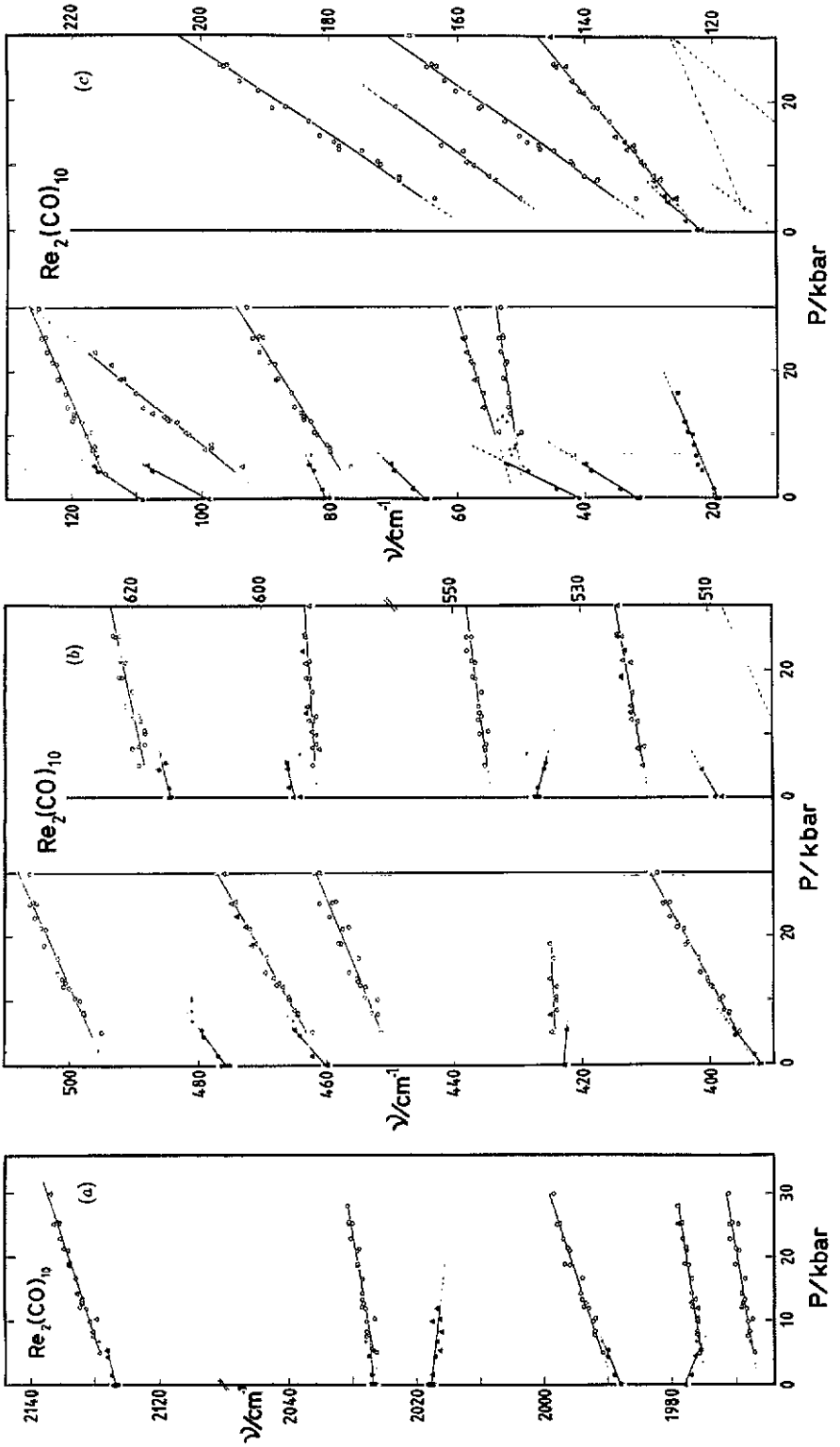


**Figure 5.** Pressure dependencies of the Raman-active modes of $Re_2(CO)_{10}$: (*a*) the $\nu$(CO) region; (*b*) the $\delta$(ReCO), $\nu$(Re–C) region; and (*c*) the deformation and lattice-mode region.

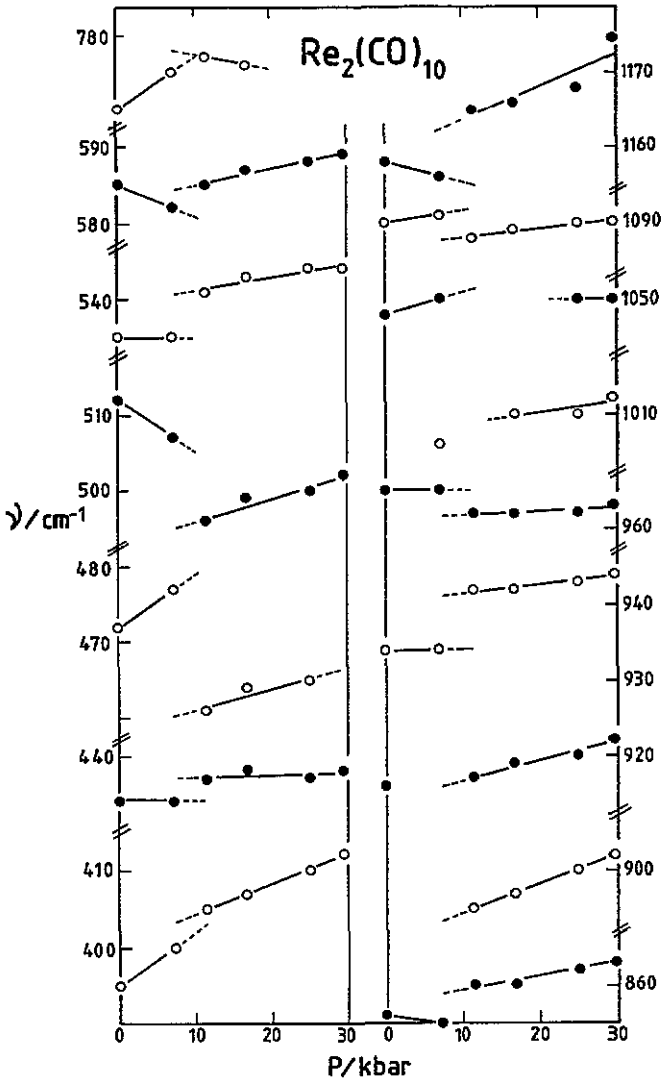


**Figure 6.** Pressure dependencies of the IR-active modes of $Re_2(CO)_{10}$ in the 380 to 1200 $cm^{-1}$ region.

Our proposal that a change of molecular geometry accompanies the phase transition in both materials is supported by the following argument. If the molecular symmetry remained $D_{4d}$ the molecules would need to be on sites in the new factor group which lifted the degeneracy of the $E_3$ but not the $E_2$ mode: the site symmetry must also be a sub-group of $D_{4d}$. No such sub-group of $D_{4d}$ has this property.

### *3.3. The δ(MCO), ν(M–C) region (350–650 $cm^{-1}$)*

Major modifications to the middle region of the spectra of both compounds accompany the phase change, figures 1 to 3. Our discussion is based upon our recent detailed reassignment using single-crystal IR (Adams and Taylor 1982) and Raman (Adams and Hooper 1979) methods.

A change from staggered to eclipsed geometry would be expected to affect

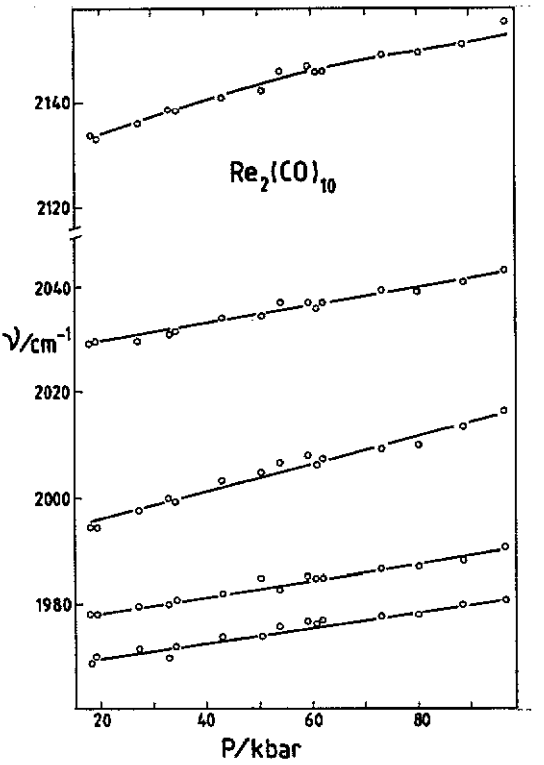


**Figure 7.** Pressure dependencies of the $\nu$(CO) modes of $Re_2(CO)_{10}$ II to 98 kbar.

**Table 1.** Raman shifts and their pressure dependencies for $Mn_2(CO)_{10}$ phase I.

| Assignment[a] | $\Delta\tilde{\nu}$ ($cm^{-1}$)[b] | $d\Delta\tilde{\nu}/dP$[c] ($cm^{-1}$ $kbar^{-1}$) | $d\ln\Delta\tilde{\nu}/dP$ ($\times10^3$ $kbar^{-1}$) |
|---|---|---|---|
| Lattice | 25.2 | 0.607 | 24 |
| modes | 37.3 | 1.791 | 44 |
| | 71.0 | 1.317 | 19 |
| $\nu_{38}$, $E_3$ | 92.2 | 1.403 | 15 |
| $\nu_7$, $A_1$ | 159.6 | 0.851 | 5.3 |
| $\nu_5$, $A_1$ | 411.4 | 1.082 | 2.6 |
| $\nu_{35}$, $E_3$ | 420.9 | 1.034 | 2.5 |
| $\nu_{34}$, $E_3$ | 465.3 | 0.666 | 14 |
| $\nu_4$, $A_1/\nu_{28}$, $E_2$ | 479.6 | 0.830 | 1.7 |
| $\nu_{26}$, $E_2$ | 673.1 | 0.541 | 0.80 |
| $\nu_{31}$, $E_3$ | 1970.3 | 0.256 | 0.13 |
| | 1980.3 | 0.075 | 0.038 |
| $\nu_2$, $A_1$ | 1990.2 | 0.450 | 0.023 |
| $\nu_{25}$, $E_2$ | 2013.4 | 0.081 | 0.040 |
| | 2022.0 | 0.318 | 0.16 |
| $\nu_1$, $A_1$ | 2115.0 | 0.437 | 0.21 |

[a] Adams and Taylor 1982, Adams *et al* 1971.
[b] Intercept at 1 bar.
[c] Slope of least-squares line.

**Table 2.** Raman shifts and their pressure dependencies for $Mn_2(CO)_{10}$ phase II.

| $\Delta\tilde{\nu}^a$ ($cm^{-1}$) | $d\Delta\tilde{\nu}/dP^b$ ($cm^{-1}$ $kbar^{-1}$) | $d\ln\Delta\tilde{\nu}/dP$ ($\times 10^3$ ($kbar^{-1}$) |
|---|---|---|
| 52.3 | 0.511 | 9.8 |
| 54.0 | 0.671 | 12 |
| 68.1 | 1.039 | 15 |
| 78.9 | 0.809 | 10 |
| 94.0 | 1.145 | 12 |
| 110.9 | 1.153 | 10 |
| 128.3 | 0.993 | 7.7 |
| 129.1 | 1.383 | 11 |
| 149.6 | 0.895 | 6.0 |
| 414.0 | 0.767 | 1.9 |
| 468.4 | 0.524 | 1.1 |
| 481.7 | 0.454 | 0.94 |
| 493.1 | 0.661 | 1.3 |
| 548.5 | 0.250 | 0.46 |
| 550.9 | 0.434 | 0.79 |
| 675.4 | 0.538 | 0.80 |
| 1969.9 | 0.357 | 0.18 |
| 1977.8 | 0.120 | 0.061 |
| 1991.1 | 0.384 | 0.19 |
| 2021.3 | 0.205 | 0.10 |
| 2115.5 | 0.391 | 0.18 |

[a] Intercept at 1 bar, for phase II this value is imaginary.
[b] Slope of least-squares line.

disproportionately the $\pi$(MCO) modes, that is those in which the equatorial carbonyl groups are deformed in directions parallel to the M–M bond. For $Re_2(CO)_{10}$ the $A_1, \nu_3$ mode is required by symmetry to be of this type, although interaction with $A_1, \nu_4, \nu$(M–C) is likely, leading to some mixing of symmetry coordinates. $\nu_3$ rises by 2.5 $cm^{-1}$ at the phase change. More dramatically, $E_3, \nu_{33}$ rises by 9 $cm^{-1}$, whereas $E_3, \nu_{32}$ drops by 4 $cm^{-1}$: the extent to which $\pi$(ReCO) bending contributes to $\nu_{33}$ rather than $\nu_{32}$ is unknown, but the high-pressure data appear to be consistent with an increase in $\pi$(ReCO) repulsion. In the IR spectrum $E_1, \nu_{19}, \pi$(ReCO) rises by 6 $cm^{-1}$. In $Mn_2(CO)_{10}$ $A_1, \nu_3$ is very weak and was not seen in the high-pressure spectra; and $E_3, \nu_{33}$ which is also weak could be seen as a doublet only in phase II.

The $\nu$(Re–C) assignment of $A_1, \nu_4$ and $\nu_5$ is firmly established on the basis of Raman solution polarization evidence. $\nu_5$ is not greatly affected by the transition but $\nu_4$ rises by no less than 17 $cm^{-1}$. $B_2$ and $A_1$ modes lie near each other in the spectra of $Mn_2(CO)_{10}$: their separation is a measure of the interaction of the two $M(CO)_5$ units across the M–M bond, via both electronic and space mechanisms. The only $B_2$ mode strong enough to be seen in the high-pressure IR spectra of $Re_2(CO)_{10}$, $\nu_{14}$, dropped by 18 $cm^{-1}$ at the transition. Hence the effect of the change of geometry on the $\nu$(Re–C) modes $\nu_4$ and $\nu_{14}$ is to increase the vibrational coupling across the molecule dramatically. Whereas under ambient conditions $\nu_4$ and $\nu_{14}$ are only 4 $cm^{-1}$ apart, at 30 kbar in phase II they are separated by 42 $cm^{-1}$.

The $E_1, \nu_{21}$ (IR), $E_2, \nu_{28}$ and $E_3, \nu_{35}$ (Raman) modes, which are all $\nu$(Re–C) equatorial modes, are little affected by the phase change. This suggests that $\nu_4$ and $\nu_{14}$, which are greatly affected, are primarily associated with Re–C(axial) bond stretching.

**Table 3.** Raman shifts and their pressure dependencies for $Re_2(CO)_{10}$ phase I.

| Assignment[a] | $\Delta\tilde{\nu}^b$ ($cm^{-1}$) | $d\Delta\tilde{\nu}/dP^c$ ($cm^{-1}$ $kbar^{-1}$) | $d\ln\Delta\tilde{\nu}/dP$ ($\times10^3$ $kbar^{-1}$) |
|---|---|---|---|
| Lattice | 19.5 | 0.411 | 21 |
| modes | 31.9 | 1.581 | 50 |
| | 40.7 | 2.053 | 50 |
| $\nu_{38}$, $E_3$ | 65.3 | 1.014 | 16 |
| $\nu_{30}$, $E_2$ | 80.6 | 0.463 | 5.7 |
| $\nu_{37}$, $E_3$ | 99.1 | 1.799 | 18 |
| $\nu_7$, $A_1$ | 109.1 | 1.466 | 13 |
| $\nu_{36}$, $E_3$ | 121.8 | 1.076 | 8.8 |
| $\nu_{35}$, $E_3$ | 392.0 | 0.803 | 2.0 |
| $\nu_{28}$, $E_2$ | 422.9 | −0.070 | −0.17 |
| $\nu_5$, $A_1$ | 460.3 | 0.912 | 2.0 |
| $\nu_4$, $A_1$ | 475.8 | 0.731 | 1.5 |
| $\nu_{26}$, $E_2$ | 508.5 | 0.574 | 1.1 |
| $\nu_{33}$, $E_3$ | 536.9 | −0.252 | −0.47 |
| $\nu_{32}$, $E_3$ | 594.9 | 0.245 | 0.41 |
| $\nu_3$, $A_1$ | 614.2 | 0.250 | 0.41 |
| $\nu_2$, $A_1$ | 1978.0 | −0.422 | −0.21 |
| $\nu_{31}$, $E_3$ | 1988.1 | 0.408 | 0.21 |
| $\nu_{25}$, $E_2$ | 2017.7 | −0.166 | −0.058 |
| | 2026.8 | 0.066 | −0.033 |
| $\nu_1$, $A_1$ | 2126.8 | 0.254 | 0.12 |

[a] Adams and Hooper 1979, Adams and Taylor 1982.
[b] Intercept at 1 bar.
[c] Slope of least-squares line.

The lower of the two $A_1$ $\nu$(CO) modes, $\nu_2$, is generally attributed to $\nu$(CO)(axial); consequently, by virtue of the familiar backbonding mechanism operative in transition-metal carbonyl compounds, the higher of the two $A_1$ $\nu$(Re–C) modes is also axial in type. The implications of these changes are considered later.

Evidence for equivalent changes in $Mn_2(CO)_{10}$ is less clear cut, partly because we have only Raman data in this case. Moreover, there are very large intensity differences between the spectra of the two parent phases themselves in this region: accordingly the two assignments are significantly different. The only really clear evidence comes from the behaviour of a band initially at 480 $cm^{-1}$ and due to near-coincidence of $A_1, \nu_4$ and $E_2, \nu_{28}$. At the phase transition a new band appeared 13 $cm^{-1}$ above the original one, which also remained. The implication is that the new band is the $A_1, \nu_4$ mode raised by increased interaction between the two ends of the molecule. The $E_2$ modes $\nu_{26-28}$ do not appear as site split doublets in the ambient phase and, hence, in contrast with the $\nu$(CO) region, give no clear evidence for change of molecular geometry.

### *3.4. The region < 250 $cm^{-1}$*

This is the region which suffers the most remarkable changes at the phase transition. This part of the spectra of both materials is of great complexity, being the superimposition of many modes, details of which have been analysed by single-crystal techniques. $Re_2(CO)_{10}$ phase II yields a Raman spectrum in this region which has the appearance of greater simplicity than that of phase I, particularly below about 100 $cm^{-1}$, implying

Table 4. Raman shifts and their pressure dependencies for $Re_2(CO)_{10}$ phase II.

| $\nu_0$ ($cm^{-1}$)[a] | $d\nu/dP$ ($cm^{-1}$ $kbar^{-1}$)[b] | $d\ln\nu/dP$ ($\times10^3$ $kbar^{-1}$) |
|---|---|---|
| 49.6 | 0.14 | 2.8 |
| 51.0 | 0.31 | 6.1 |
| 75.5 | 0.64 | 8.4 |
| 89.5 | 1.23 | 13 |
| 113.4 | 0.44 | 3.9 |
| 122.0 | 0.86 | 7.0 |
| 127.7 | 1.46 | 11 |
| 143.1 | 1.43 | 10 |
| 157.7 | 1.53 | 9.7 |
| 393.1 | 0.53 | 1.4 |
| 424.1 | 0.04 | 0.1 |
| 449.6 | 0.39 | 0.9 |
| 460.5 | 0.55 | 1.2 |
| 494.4 | 0.45 | 0.9 |
| 519.4 | 0.17 | 0.3 |
| 617.1 | 0.21 | 0.3 |
| 1966.5 | 0.16 | 0.08 |
| 1974.4 | 0.16 | 0.08 |
| 1989.3 | 0.33 | 0.16 |
| 2026.0 | 0.17 | 0.08 |
| 2127.5 | 0.33 | 0.16 |

[a] Intercept at 1 bar: this value is imaginary.
[b] The initial slope of the line is given. Above about 40 kbar nearly all the plots become non-linear.

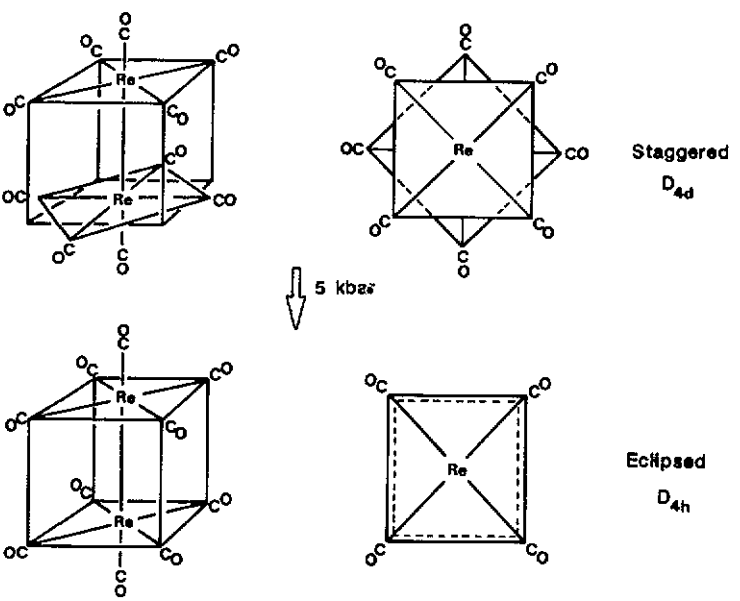


Figure 8. The proposed molecular rearrangement of $Re_2(CO)_{10}$.

that the new cell has higher symmetry than monoclinic, possible orthorhombic. It is unlikely that the primitive cell content has changed.

**Table 5.** Distribution and numbering of modes for $D_{4d}$ $M_2(CO)_{10}$ (Adams and Hooper 1979).

| | | | |
|---|---|---|---|
| $A_1$ (Raman-active) | | $E_1$ (IR-active) | |
| $\nu_1$ | $\nu$(CO) equatorial | $\nu_{17}$ | $\nu$(CO) equatorial |
| $\nu_2$ | $\nu$(CO) axial | $\nu_{18}$ | $\delta$(MCO) |
| $\nu_3$ | $\pi$(MCO) | $\nu_{19}$ | $\pi$(MCO) |
| $\nu_4$ | $\nu$(M–CO) | $\nu_{20}$ | $\rho$(MCO) axial |
| $\nu_5$ | $\nu$(M–CO) | $\nu_{21}$ | $\nu$(M–CO) equatorial |
| $\nu_6$ | $\pi$(CMC) | $\nu_{22}$ | $\delta$(CMC) |
| $\nu_7$ | $\nu$(M–M) | $\nu_{23}$ | $\pi$(CMC) |
| | | $\nu_{24}$ | $\Delta$ |
| $A_2$ (inactive) | | | |
| $\nu_8$ | $\delta$(MCO) | $E_2$ (Raman-active) | |
| | | $\nu_{25}$ | $\nu$(CO) equatorial |
| $B_1$ (inactive) | | $\nu_{26}$ | $\delta$(MCO) |
| $\nu_9$ | $\delta$(MCO) | $\nu_{27}$ | $\pi$(MCO) |
| $\nu_{10}$ | Torsion | $\nu_{28}$ | $\nu$(M–CO) equatorial |
| | | $\nu_{29}$ | $\delta$(CMC) |
| $B_2$ (IR-active) | | $\nu_{30}$ | $\pi$(CMC) |
| $\nu_{11}$ | $\nu$(CO) equatorial | | |
| $\nu_{12}$ | $\nu$(CO) axial | $E_3$ (Raman-active) | |
| $\nu_{13}$ | $\pi$(MCO) | $\nu_{31}$ | $\nu$(CO) equatorial |
| $\nu_{14}$ | $\nu$(M–CO) | $\nu_{32}$ | $\delta$(MCO) |
| $\nu_{15}$ | $\nu$(M–CO) | $\nu_{33}$ | $\pi$(MCO) |
| $\nu_{16}$ | $\pi$(CMC) | $\nu_{34}$ | $\rho$(MCO) axial |
| | | $\nu_{35}$ | $\nu$(M–CO) equatorial |
| | | $\nu_{36}$ | $\delta$(CMC) |
| | | $\nu_{37}$ | $\pi$(CMC) |
| | | $\nu_{38}$ | $\Delta$ |

Two $A_1$ modes lie in this region. For $Mn_2(CO)_{10}$ it is known that they are respectively: 160 $cm^{-1}$, $\nu_6$, $\nu$(Mn–Mn) and 116 $cm^{-1}$, $\nu_7$, $\delta$(CMnC). However, although the symmetry labelling of the analogous modes of $Re_2(CO)_{10}$ is not in doubt (129, 109 $cm^{-1}$), the extent of the $\nu$(Re–Re) contribution to each is not settled beyond dispute. At the phase transition it is these two modes which suffer the greatest changes in that their relative intensities are dramatically reversed. Almost the same thing happens in $Mn_2(CO)_{10}$: $\nu_7$ gains intensity significantly although $\nu$(Mn–Mn) does not lose it concurrently. These observations are difficult to account for other than on the basis of a modification of electronic structure.

### *3.5. The electronic changes*

Our data are consistent with (indeed, require) a change of molecular geometry from $D_{4d}$ to $D_{4h}$ at the phase transition. The mode shifts show that this change is accompanied by increased metal to carbonyl backbonding to the axial but not the equatorial groups. Thus, for $Re_2(CO)_{10}$, $\nu$(CO), $(A_1, \nu_2)$ drops 8 $cm^{-1}$ whilst $\nu$(Re–C), $(A_1, \nu_4)$ rises by 17 $cm^{-1}$. Concurrently, major intensity changes occur in the low-frequency region and, at the very least, indicate modification of the Re–Re bond.

There have been many theoretical studies of the bonding in the title compounds but there seems to be little disagreement with the view expressed by Freund and Hohlneicher (1979) the '$\pi$-interaction does not contribute to metal–metal bonding in unbridged CO clusters'. However, Carroll *et al* (1985) from a study of the $\sigma \rightarrow \sigma*$ transition associated with the metal–metal bond showed that the main effect of

**Table 6.** Unit cell relationships for the ambient phase structure of $M_2(CO)_{10}$.

| Molecular symmetry | Site symmetry | Unit cell symmetry |
|---|---|---|
| $D_{4d}$ | $C_2(C_{2'})$ | $C_{2h}^6$ |

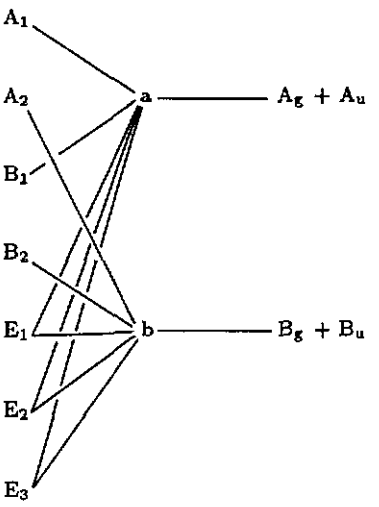


**Table 7.** Symmetry relationships and Raman activities for the $D_{4h}$ and $D_{4d}$ structures.

| $D_{4d}$ ← x2 | $C_{4v}$ | x2 → $D_{4h}$ |
|---|---|---|
| $A_1^* + B_2$ | $A_1$ (axial) | $A_{1g}^* + A_{2u}$ |
| $A_1^* + B_2$ | $A_1$ (equatorial) | $A_{1g}^* + A_{2u}$ |
| $E_2^*$ | $B_1$ | $B_{1g}^* + B_{2u}$ |
| $E_1 + E_3^*$ | E | $E_g^* + E_u$ |

* Raman active.

pressure (to 120 kbar) upon the electronic spectra of both compounds is to stabilize the $\sigma$- relative to the $\sigma*$-orbital by virtue of increased orbital overlap.

We have demonstrated a remarkable increase in the coupling of the $\nu$(Re–C) axial modes $\nu_4$ and $\nu_{14}$ across the Re–Re bond at the phase change. There are two mechanisms which may contribute to such a change: mechanical coupling and electronic coupling. It is most unlikely that this magnitude of change could be accounted for by the likely decrease in the Re–Re bond length at the phase transition, but it can reasonably be associated with overlap of metal $d_{xz}$ orbitals across the Re–Re bond and with the carbonyl $\pi^*$-orbitals at either end of the molecule. The compression accompanying the phase change must be sufficient to bring about $d_{xz}$–$d_{xz}$ overlap.

A change from $D_{4d}$ to $D_{4h}$ molecular symmetry suggests that the torsional mode is implicated in the phase transition. However, this is unlikely to be the soft mode which drives the transition as this would need to transform into a totally symmetric mode in the new structure. More probably it will be found to be coupled with a lattice mode.

Neither material undergoes a phase change upon cooling to low temperature (Mn 74 K (Martin *et al* 1982), Re 67 K (Harvey and Butler 1985)), but the dihedral angle (45° for strict $D_{4d}$ molecular symmetry) increases from 47.4° at room temperature to 50.2° at 74 K (Martin *et al* 1982). The possibility exists that the I/II phase boundary may intersect the temperature axis below this value. The mechanism of this transition warrants further study, especially by inelastic neutron scattering.

## Acknowledgment

We thank the SERC for maintenance grants to PDH and ACS, and for other support.

## References

Adams D M, Appleby R and Sharma S K 1976 *J. Phys. C: Solid State Phys.* **21** 623–37
Adams D M, Hatton P D, Shaw A C and Tan T-K 1981 *J. Chem. Soc., Chem. Commun.* 226–7
Adams D M and Hooper M A 1979 *J. Organometall. Chem.* **181** 131–41
Adams D M and Taylor I D 1982 *J. Chem. Soc., Faraday Trans.* **78** 1065–90
Carroll T L, Shapley J R and Drickamer H G 1985 *Chem. Phys. Lett.* **119** 340–3
Churchill M R, Amoh K N and Wasserman M J 1981 *Inorg. Chem.* **20** 1609–11
Cotton F A and Troup J M 1974 *J. Chem. Soc., Dalton Trans.* 800–4
Dahl L F, Ishii E and Rundle R E 1957 *J. Chem. Phys.* **26** 1750–71
Freund H-J and Hohlneicher G 1979 *Theor. Chim. Acta* **51** 145–62
Harvey P D and Butler I S 1985 *Can. J. Chem.* **63** 1510–7
Martin M, Rees B and Mitschler A 1982 *Acta Crystallogr.* B **38** 6–15
Ponte-Goncalves A M 1980 *Progr. in Solid State Chem.* **13** 1
Powell H M and Evans R V G 1939 *J. Chem. Soc.* 286